

# A Simulation Method for Temperature Monitoring of Medium Voltage Underground Cables Insulation

Quyem M. Hoang<sup>1</sup>, Hai D. Tran<sup>1</sup>, and Nga T. T. Vu<sup>2,\*</sup>

<sup>1</sup> Faculty of Electrical Engineering, School of Electrical and Electronic Engineering, Hanoi University of Industry, Hanoi, Vietnam

<sup>2</sup> Faculty of Electrical Engineering, Electric Power University, Hanoi, Vietnam

Email: quyehm@hau.edu.vn (Q.M.H.), tranduchaidh07@gmail.com (H.D.T.), ngavtt@epu.edu.vn (N.T.T.V.)

Manuscript received February 24, 2025; revised April 10, 2025; accepted May 11, 2025

\*Corresponding author

**Abstract**—Temperature is one of the primary causes of medium voltage cable failures. When the temperature exceeds the allowable limit, the cable components may degrade, affecting the lifespan and operational efficiency of the power system. In order to maintain the safe operation of power systems and minimize the likelihood of severe accidents, it is crucial to analyze the temperature distribution in medium voltage underground cables. In this study, the time-dependent temperature distribution within the 5.5 mm thick Cross-Linked Polyethylene (XLPE) insulation layer of medium voltage cables is analyzed using the finite element method. Temperature data collected from the cable sheath surface is utilized to simulate the thermal variation in cable insulation layer under the varying of core current and sheath temperature. Additionally, a temperature warning threshold is calculated to issue alerts and prevent overheating. The variations in the electric field under these conditions are also examined. The results provide valuable insights for optimizing the installation and operation of medium voltage power cables.

**Index Terms**—monitoring, Medium Voltage (MV) underground cable, reliability, temperature distribution, Cross-Linked Polyethylene (XLPE)

## I. INTRODUCTION

As economies continue to grow, the demand for a reliable power supply is rising, placing new challenges on the operation and maintenance of power distribution management units. Medium Voltage (MV) underground cables play a critical role in the transmission and distribution system, ensuring the stability and safety of the power grid. However, one of the most significant challenges affecting MV underground cables is the rise in operating temperature, which can severely impact their performance and lifespan.

The estimation of the operating temperature of the Cross-Linked Polyethylene (XLPE) insulation relies on data obtained from the cable sheath. The temperature distribution within the insulation layer is a key factor in determining both the longevity of the cable material and the overall reliability of the power system. Prolonged exposure to temperatures exceeding the allowable limit

can lead to the breakdown of the molecular structure of the insulation, accelerating its degradation [1–4]. As a result, continuous monitoring of the XLPE insulation temperature is essential, as it directly influences the operational performance and durability of the entire underground cable network. This assertion has been further validated in a study by Smaida *et al.* [5]

Furthermore, the XLPE insulation layer is positioned near the conductor, which serves as the primary heat source within the cable. Under high-temperature conditions, space charge accumulation within the polymer material leads to an uneven electric field distribution, increasing the likelihood of microscopic defects such as electrical trees. These defects propagate more rapidly as temperatures rise, further deteriorating insulation properties, shortening the service life of the cable, and potentially resulting in failure under prolonged high-voltage operation [6]. Consequently, maintaining optimal XLPE temperature levels is crucial for ensuring a uniform electric field distribution around the cable and preventing premature degradation.

To address these concerns, various methods for monitoring and diagnosing insulation faults have been explored. In reference [7], by simulating various levels of insulation degradation, data are gathered regarding the surface temperature rise behavior of the cable and the correlation between temperature elevation and the severity of insulation damage. To estimate the conductor's dynamic temperature, the model utilizes the measured cable surface temperature and load current as input variables. However, implementing this approach necessitates a substantial dataset for effective training of the temperature prediction model [8]. Numerical calculation methods have also been used to assist in the comprehensive monitoring of cable temperatures. Factors affecting cable temperature include load current, environmental conditions, cable material structure, and heat dissipation in the surrounding environment. Direct measurement of conductor temperature in in-service cables presents significant challenges; hence, it is commonly estimated through analytical models. However, these models often neglect the influence of external

environmental variations and fail to account for complex physical phenomena such as air convection, radiation, and coupled heat transfer processes. As a result, the calculated temperatures may significantly deviate from actual values in complex and multi-loop systems, limiting the applicability of such methods for real-time conductor temperature monitoring. Therefore, it can be confirmed that studies on cable temperature analysis typically focus on monitoring surface or conductor temperatures, whereas the temperature of the insulation layer has not been adequately addressed. Monitoring the cable insulation layer temperature requires higher costs and advanced technology.

To address these issues, a method for monitoring underground cable temperatures based on the use of cable sheath temperature sensors has demonstrated the ability to monitor temperatures effectively and continuously, especially when combined with detailed simulation of the temperature distribution of XLPE insulation. The close correlation between cable sheath temperature and XLPE insulation temperature can be exploited to provide early warnings of overheating, minimizing risks and improving the reliability of the cable system. The advantage of this method is that the temperature sensor placed on the cable sheath simplifies the installation and maintenance process while minimizing interference with the internal structure of the cable. Through simulations using the Finite Element Method (FEM), the insulation temperature can be calculated in detail and accurately from the cable sheath temperature data, ensuring the accuracy of temperature measurements and the effectiveness of the warning system, helping to monitor the operating conditions of the cable more comprehensively without direct contact with the internal structure of the cable.

The study also examines the variations in the electric field under these conditions. The findings offer valuable insights for optimizing the installation and operational conditions of medium voltage power cables.

## II. HEAT TRANSFER AND ELECTRIC FIELD MODEL IN MEDIUM VOLTAGE CABLE

In heat transfer models, MV underground cables are typically assumed to have infinite length to simplify calculations and analysis. When current passes through the conductor, it generates heat, resulting in a complex diffusion process within the cable. Current studies on temperature distribution in underground cables mainly focus on radial heat transfer in a Two-Dimensional (2D) space, as heat primarily dissipates outward from the conductor to the cable sheath [9–11]. The temperature gradually decreases from the conductor, where the highest temperature appears, to the outside, through the material layers, and continues to decrease when transferred to the air. Therefore, the radial heat transfer has a great influence on the cooling efficiency of underground cables. Temperature monitoring and maintaining a safe temperature threshold for cable insulation are essential to ensure the reliability and stability of the line.

The main components of MV underground cable lines include cable sections which are connected by cable joints when it is necessary to transmit and distribute electricity over large distances. MV underground cables are composed of one or more cores and many layers of materials. The selection of the type and structure of MV underground cables will depend on the requirements and specific operating conditions of the line. In this study, the authors performed on a single-core MV underground cable of CADIVI, with the basic structure shown in Fig. 1.

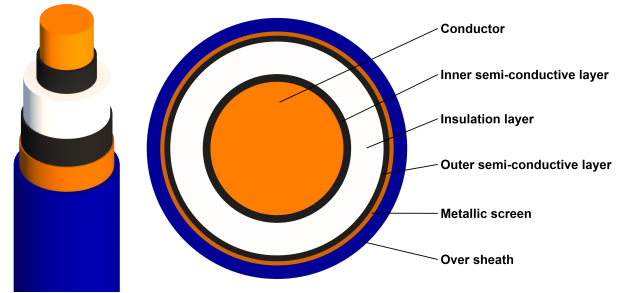


Fig. 1. Structure of single-core MV underground cable.

The insulation material in underground cables is affected by the electric field, depending on the applied voltage level, causing dielectric losses within the cable. In addition, eddy currents may arise on the ground shield of the cable. If the shield is made of magnetic material, additional losses due to hysteresis and eddy currents will also occur, increasing energy loss and heat generation in the cable system.

The main cause of heating in the electric cable is the loss of electrical energy over time  $t$ . This heat, converted from electrical energy, dissipates into the environment from the conductor. Based on Fourier's law, the heat transfer process is governed by the differential equation presented in Eq. (1) [12].

$$\nabla \cdot (k \nabla T) + q_v = \rho c \frac{\partial T}{\partial t}. \quad (1)$$

In this equation,  $T$  denotes the temperature variable (K),  $k$  denotes the thermal conductivity (W/m.K),  $\rho$  represents the material density ( $\text{kg}/\text{m}^3$ ),  $c$  refers to the specific heat capacity of the heat transfer medium ( $\text{J}/\text{kg.K}$ ),  $q_v$  corresponds to the volumetric heat source intensity ( $\text{W}/\text{m}^3$ ). The thermal conductivity  $k$  characterizes the relationship between the heat flux vector  $q$  and the temperature gradient  $\nabla T$  as described by the corresponding mathematical expression  $q = -k \nabla T$ .

In the isothermal state, the right-hand side of Eq. (1) disappears, the temperature distribution is given by the Poisson equation, and the conditions for the temperature limit (Dirichlet condition) or heat flux (Neumann condition):  $\nabla \cdot (k \nabla T) + q_v = 0$ .

Under steady-state conditions in a two-dimensional thermal system, Eq. (1) takes a simplified form:

$$\frac{\partial}{\partial x} \left( k \frac{\partial T}{\partial x} \right) + \frac{\partial}{\partial y} \left( k \frac{\partial T}{\partial y} \right) = -q_v. \quad (2)$$

Eq. (2) can be solved to determine the temperature at any point within any homogeneous region with specified heat conduction and heat generation rate based on the defined boundary conditions.

In the analysis, volumetric heat flux plays an essential role, providing a measure of thermal energy transfer density within the cable conductor, as demonstrated in Eq. (3).

$$Q_b(T_c) = \frac{P_b}{A}. \quad (3)$$

where  $A$  is the geometric cross-sectional area of the conductor ( $m^2$ ), and  $P_b$  is the heat loss of the cable (W/m) which can be calculated through the equation below:

$$P_b = I^2 R_{ac}. \quad (4)$$

The AC resistance of a cable conductor differs from its DC resistance due to additional effects that arise under alternating current. Specifically, when two adjacent cables carry AC current, phenomena such as the skin effect and proximity effect become significant, leading to an increase in AC resistance. According to IEC 60287-1-2 [13], the AC resistance can be represented as a function of the DC resistance, modified by corresponding correction factors that account for the skin and proximity effects, as described by Eq. (5).

$$R_{ac} = R_{dc} (1 + \gamma_s + \gamma_p). \quad (5)$$

In this equation,  $R_{ac}$  denotes the alternating current (AC) resistance of the conductor per unit length ( $\Omega/m$ ), while  $R_{dc}$  represents the direct current (DC) resistance per unit length ( $\Omega/m$ ) at temperature  $T$ , which can be determined using (6).

$$R_{dc} = R_{ref} [1 + \alpha_{ref} (T(x, y) - T_{ref})]. \quad (6)$$

Here,  $R_{ref}$  and  $\alpha_{ref}$  denote the reference resistance of the cable conductor ( $\Omega$ ) and the temperature coefficient of the conductor material ( $1/K$ ), respectively, both defined at the reference temperature  $T_{ref} = 20$  °C. The operating temperature of the conductor is represented by  $T(x, y)$ . The reference resistance of the conductor can be calculated using the Eq. (7).

$$R_{ref} = \rho_{20} / A. \quad (7)$$

We have  $\gamma_s$  and  $\gamma_p$  as the skin effect and proximity effect coefficients, respectively, as defined by IEC 60287-1-2 [13]:

$$\gamma_s = \frac{x_s^4}{192 + 0.8x_s^4}. \quad (8)$$

where:

$$x_s^2 = \frac{8\pi f}{R_{dc}} 10^{-7} k_s. \quad (9)$$

$$\gamma_p = \frac{x_p^4}{192 + 0.8x_p^4} \left( \frac{d_c}{s} \right)^2 \left[ 0.312 \left( \frac{d_c}{s} \right)^2 + \frac{1.18}{\frac{x_p^4}{192 + 0.8x_p^4} + 0.27} \right]. \quad (10)$$

$$x_p^2 = \frac{8\pi f}{R_{dc}} 10^{-7} k_p. \quad (11)$$

Here,  $f$  denotes the frequency of the alternating current flowing through the conductor (Hz),  $d_c$  is the conductor diameter (m), and  $s$  represents the center-to-center spacing between adjacent conductors (m). The variables  $x_s$  and  $x_p$  are the arguments of the Bessel functions employed in the calculation of the skin and proximity effects, respectively,  $k_s$  and  $k_p$  serve as the corresponding correction factors for these effects.

When performing heat transfer model calculations and assuming that the MV underground cable is new and free of defects or damage, it is essential to define the appropriate boundary conditions. In this study, two main types of boundary conditions are considered:

- 1) Fixed Temperature Boundary Condition: The temperature at the boundary is known and remains constant. In the simulation, this temperature value is obtained from a sensor located at the cable sheath. The model incorporates both convective and radiative heat transfer by integrating these effects into the temperature boundary condition derived from the sensor readings.
- 2) Heat Flux Boundary Condition: The current flowing through the conductor governs the resulting power loss, taking into account the influences of both skin and proximity effects. This power loss is then used to calculate the corresponding heat flux at the boundary.

Boundary temperature at constant value:

$$T|_r = T_s. \quad (12)$$

where  $T_s$  is the boundary temperature (K), which is kept constant. The boundary condition for the soil layer considered in the article is that of the deep soil layer, with a temperature of 20 °C.

Heat flow density at the boundary via phase method:

$$-\lambda \frac{\partial T}{\partial n} \Big|_r = q_w. \quad (13)$$

where  $\lambda$  denotes the thermal conductivity of the material (W/m.K) and  $q_w$  represents the heat flux density (W/m<sup>2</sup>).

The electric field is the spatial derivative of the voltage. The conductivity, one input parameter of the model, is as a function of electric field and temperature and fitted to a law of the type [14]:

$$\sigma(T, E) = A \exp\left(\frac{-E_a}{k_B T}\right) \sin h[(aT + b)E] E^\alpha. \quad (14)$$

In the equation,  $\sigma$  refers to electrical conductivity (S/m),  $E$  is the applied electric field (V/m),  $E_a$  corresponds to the activation energy (eV),  $k_B$  is the Boltzmann constant (eV/K), and other coefficients. The coefficient values are reported in Table I.

TABLE I: COEFFICIENT VALUES IN (14) DESCRIBING THE CONDUCTIVITY OF XLPE AS A FUNCTION OF ELECTRIC FIELD AND TEMPERATURE

Parameter	Value
$A$	0.8
$E_a$ (eV)	1.0
$k_B$ (eV/K)	$8.62 \cdot 10^{-5}$
$a$ (m/V/K)	0 if $T < 313$ K; $-1.3 \cdot 10^{-9}$ if $T \geq 313$ K
$b$ (m/V)	$1.38 \cdot 10^{-7}$ if $T < 313$ K; $5.45 \cdot 10^{-7}$ if $T \geq 313$ K
$\alpha$	0.15

### III. NUMERICAL METHOD AND CABLE SAMPLE

For thermal analysis of underground cables, FEM is employed as a numerical approach. Using COMSOL Multiphysics 6.2 software, the temperature distribution is calculated under different temperature conditions at the cable sheath. The first step of this method involves

constructing a geometric model of cable material. The cable specifications and material properties used in the simulation are based on the data listed in Table II. The simulation was achieved in 2D in time with the external ambient temperature and the reference temperature for the material are assumed to be 20°C [13]. In the simulation, radiation and natural convection heat transfer were taken into account.  $T_s$  value is the measured temperature of sensors in the monitoring system.

The simulation set at an applied voltage of 24 kV, temperature distribution in the cable was calculated under various operating conditions of two main parameters: current flowing through the conductor (from 200 A to the permissible current value of the studied cable, which is 590 A [15]) and the temperature value obtained from the temperature sensor placed at the cable sheath ( $T_s$ ) in the range from 30°C to 85°C in increments of 5°C. From the variation of temperature on the voltage insulation layer, the electric field value in the insulation layer is also calculated and analyzed.

TABLE II: TECHNICAL SPECIFICATIONS AND MATERIAL PROPERTIES OF MV UNDERGROUND CABLES, VOLTAGE LEVEL 12/20 (24) kV OR 12.7/22 (24) kV [16–18]

Structure	Thickness (mm)	Material	Thermal conductivity $k$ (W/m.K)	Specific heat capacity $c$ (J/kg.K)	Density $\rho$ (kg/m <sup>3</sup> )	Conductivity $\sigma_{20}$ at 20°C (S/m)	Resistivity $\rho_{20}$ at 20°C ( $\Omega$ .m)
Conductor	11.3	Copper	400	385	8940	$5.96 \cdot 10^7$	$1.68 \cdot 10^{-8}$
Inner semi-conductor layer	1.3	Semiconductor compound (polyethylene mixed with carbon black)	0.2875	2200	940	$5.998 \cdot 10^3$	$1.667 \cdot 10^{-4}$
Insulation layer	5.5	XLPE	0.2875	2526	1200	$\sigma(T, E)$ of material	-
Outer semi-conductor layer	1.0	Semiconductor compound (polyethylene mixed with carbon black)	0.2875	2200	940	$5.998 \cdot 10^3$	$1.667 \cdot 10^{-4}$
Metallic screen	0.7	Copper	400	385	8940	$5.96 \cdot 10^7$	$1.68 \cdot 10^{-8}$
Over sheath	2.3	HDPE	0.2875	2200	950	-	-

## IV. RESULTS AND DISCUSSION

### A. Temperature and Electric Field Distribution in the Cable over Time

The simulation results of temperature distribution in the MV cable test sample with a conductor current of  $I = 400$  A and an sheath temperature of  $T_s = 30^\circ\text{C}$  at different time intervals, are presented in Fig. 2. Fig. 2 (a) illustrates the temperature distribution on a two-dimensional cross-section of the cable at 24 hours after the application of voltage. The distribution is radially symmetric with respect to the center of the cable. To facilitate data analysis, one-dimensional temperature profiles in Fig. 2 (b) were extracted from the 2D plot for comparison and further evaluation. The same approach was utilized in the electric field distribution results.

The temperature characteristics remain almost unchanged or reach a steady state after 6 hours. The graph reflects the uneven temperature distribution in the cable, showing the temperature change at each material layer and the heat transfer mechanism according to the radial radius. After 6 hours, the maximum temperature at the cable insulation ( $T_{\max}$ ) reaches about  $32.07^\circ\text{C}$ . The

simulation results reveal a symmetrical temperature distribution within the cable. Therefore, temperature monitoring should account for this symmetry to ensure that no localized hotspots develop within the cable structure. The large temperature difference between the material layers reflects the nonlinear heat transfer properties along the radial radius. The material layers that make up the cable affect the heat transfer, regulation, and distribution of the heat generated from the cable conductor. Heat is transferred to the surroundings via the thermal conductivity of the material layers, thereby reducing the temperature in the cable gradually and continuously without causing heat accumulation in the cable structure.

The electric field changes due to variation of temperature in the insulation layer of the cable, (Fig. 3 (a)). When  $T_s = 30^\circ\text{C}$ , the current in core is  $I_{\text{core}} = 400$  A (the gradient of temperature between the inner core and outer interface is  $2.5^\circ\text{C}$ ), the simulation results indicate a temporal shift in the electric field distribution across the cable insulation. Specifically, the electric field intensity near the conductor gradually decreases from 4.8 kV/mm to 4.4 kV/mm over a 24-hour period, while an opposite trend is observed at the outer interface of the insulation

and semiconducting layer, where the field increases from 3.35 kV/mm to 3.65 kV/mm. This behavior suggests a redistribution of the electric field within the insulation structure.

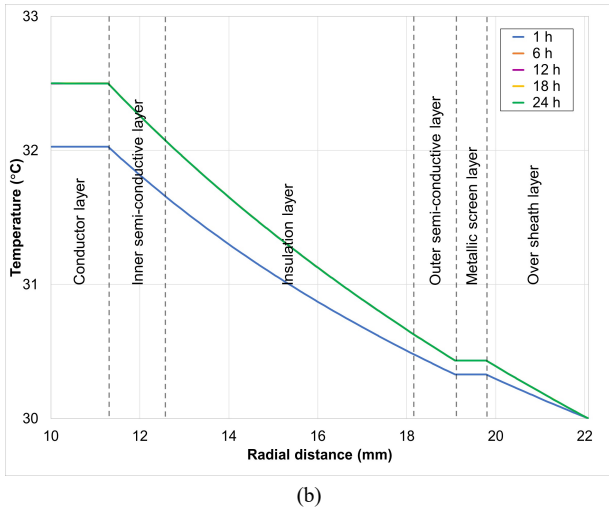
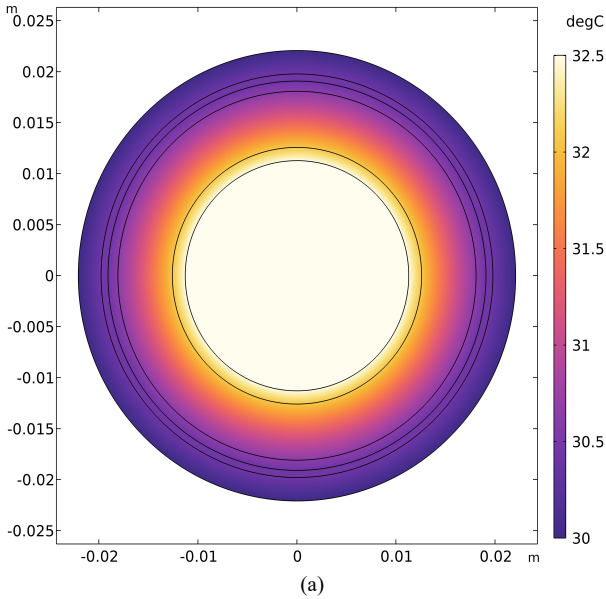


Fig. 2. Temperature distribution in MV cable when  $I_{core} = 400$  A and  $T_s = 30^\circ\text{C}$ : (a) 2D cross-section at 24h and (b) 1D at different times.

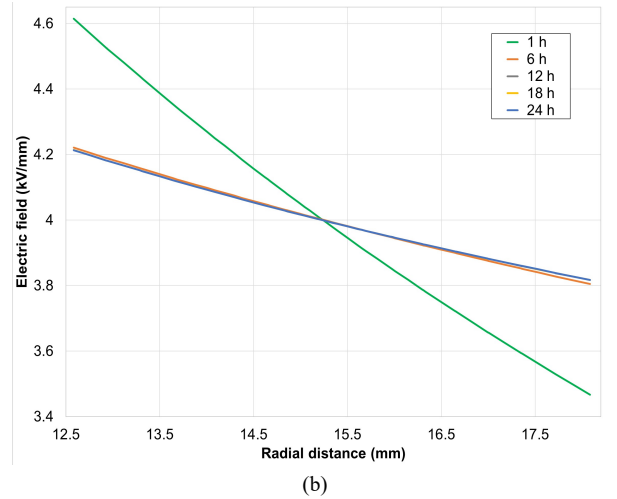
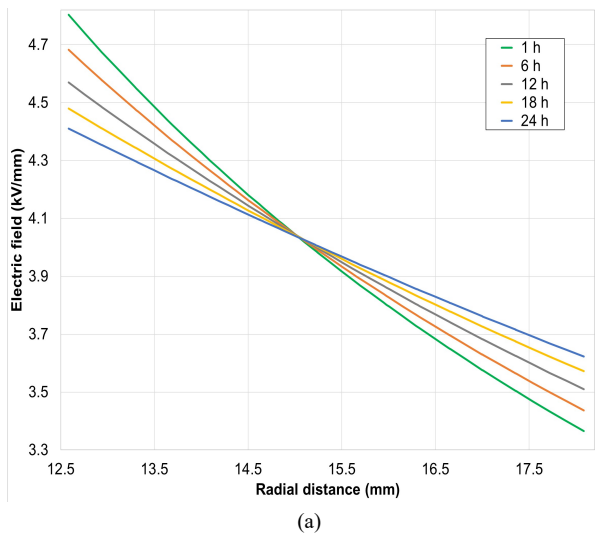


Fig. 3. Variation of the electric field in the XLPE layer cable at different times after applying voltage when  $I_{core} = 400$  A: (a)  $T_s = 30^\circ\text{C}$  and (b)  $T_s = 60^\circ\text{C}$ .

Notably, the system does not reach electrostatic equilibrium within 24 hours, implying that further evolution of the electric field is expected beyond this time frame. When  $T_s = 60^\circ\text{C}$ , the field profiles of Fig. 3 (b) show decreasing trends in time at inner and increasing at outer interface of insulation. The value of electric field achieves 4.2 kV/mm and 3.8 kV/mm respectively inner and outer interface of insulation after 6 hours of operation, then the value does not change much and reaches the steady state at 24 hours.

Thus, temperature greatly affects the change in electric field, this process is difficult to predict. When the temperature increases, it leads to large electric field variations in the cable insulation layer, causing the cable life to decrease rapidly, possibly leading to cable failure.

This phenomenon of the electric field arises because the conductivity is non-linear with the field. As a result, it counteracts the temperature effect on the conductor. In the next simulations, we use temperature characteristics at steady state to analyze.

### B. Temperature Distribution in the Cable at Different Cable Surface Temperatures

Fig. 4 presents the temperature distribution along the radial direction of the medium-voltage underground cable operating at the allowable current threshold of 590 A, with the surface temperature  $T_s$  varying from  $30^\circ\text{C}$  to  $85^\circ\text{C}$ . When  $T_s$  increases, the temperature gradient of  $T_{max}$  and  $T_s$  also rises, ranging from  $5.5^\circ\text{C}$  to  $6.5^\circ\text{C}$ . This shows the influence of the temperature  $T_s$  on the temperature difference between  $T_s$  and  $T_{max}$ . Therefore, when underground cables are designed to operate under high load conditions or in places with harsh ambient temperatures, special attention must be paid to the calculation and monitoring the cable's temperature distribution. This shows that the thermal conductivity  $k$  and the thickness of the material layer significantly influence heat dissipation, particularly in the XLPE insulation layer. Furthermore, the temperature increase reflects the presence of heat loss and dielectric loss in the material layer of the cable.

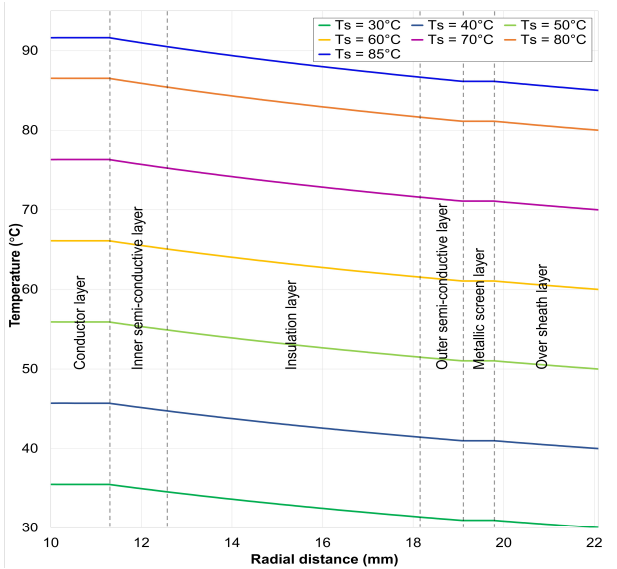


Fig. 4. Temperature distribution in the MV cable when  $I_{\text{core}} = 590$  A with different  $T_s$  values.

It can be seen that under the same current level, the increase in temperature  $T_{\text{max}}$  is almost linear with the increase in temperature  $T_s$ . According to the study [19], the temperature distribution in underground cables is determined by the total thermal resistance of the material layers. Although the intermediate layers have different thermal conductivity properties, the total thermal resistance of the entire system still maintains a linear relationship. At this time, the total thermal resistance acts as a thermal bridge, ensuring that a steady heat transfer from the cable conductor to the cable sheath is maintained, resulting in a linear relationship between  $T_s$  and  $T_{\text{max}}$ . In addition, according to IEC 60287-2-1 [13], the method of calculating the total thermal resistance has confirmed the correctness of the linear model when evaluating the  $T_{\text{max}}$  value based on the  $T_s$  value. The nearly linear relationship between  $T_s$  and  $T_{\text{max}}$  is influenced by the constant current level, combined with stable boundary conditions during the simulation process, which helps to limit unwanted temperature fluctuations.

The relationship between the temperature value  $T_s$  and the temperature  $T_{\text{max}}$ , when  $I = 590$  A at different  $T_s$  values is shown in Fig 5. The simulation results using the numerical method are shown by the blue dotted points, while the linear regression line determines the correlation between the  $T_s$  and  $T_{\text{max}}$  values, shown by the orange straight line.

The linear regression equation showing the correlation between the  $T_s$  and  $T_{\text{max}}$  is represented as:

$$T_{\text{max}} = aT_s + b. \quad (15)$$

where the parameter  $a$  reflects the variation of temperature  $T_{\text{max}}$  with the change of temperature  $T_s$ . The value of  $a$  determines the slope of the linear regression equation and is affected by the operating current level, which is clearly shown by the increase in the slope of the linear line when the current is larger. The value of  $b$  is a constant representing the initial difference between  $T_{\text{max}}$  and  $T_s$ , usually due to the non-instantaneous radial heat

transfer from the conductor to the cable jacket. The initial difference is affected by factors such as the structure of the insulation layer, the thermal conductivity of the material, and the ambient conditions of the cable.

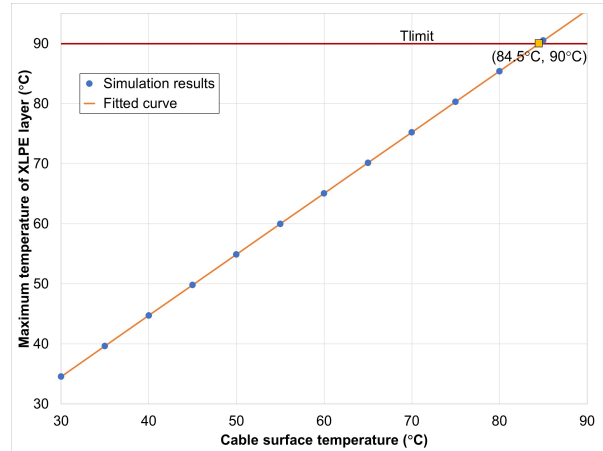


Fig. 5. The relationship between the temperature  $T_s$  and the temperature  $T_{\text{max}}$ , when  $I_{\text{core}} = 590$  A with different  $T_s$  values.

The accuracy of the method is checked by calculating the error between the  $T_{\text{max}}$  value obtained from the linear equation and the  $T_{\text{max}}$  result obtained from the simulation model. The largest relative error between the two  $T_{\text{max}}$  values is relatively small, about 0.002%, occurring at  $T_s = 50^\circ\text{C}$ . Based on the simulation results in Fig. 6, the intersection point between the linear regression line and the  $T_{\text{limit}}$  axis can indicate the coordinates of the pair of temperature values ( $T_{\text{max}}, T_s$ ) as ( $84.5^\circ\text{C}, 90^\circ\text{C}$ ). This is the point that determines the temperature value  $T_s$  when the cable insulation temperature reaches the fault threshold. Thereby, when the cable operates with a rated current of 590 A and the maximum temperature value of the cable insulation  $T_{\text{limit}} = 90^\circ\text{C}$  for XLPE insulated cables [20, 21], an alarm will need to be issued when the sensor temperature at the cable sheath reaches the threshold value  $T_s = 84.5^\circ\text{C}$ .

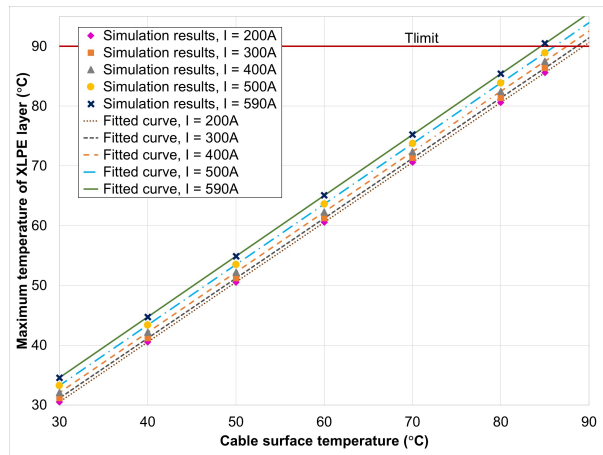


Fig. 6. The relationship between the temperature  $T_s$  and  $T_{\text{max}}$  depends on the current  $I_{\text{core}}$  and temperature  $T_s$ .

### C. Temperature Warning Threshold Determination

Fig. 6 shows the relationship between the temperature value  $T_s$  and  $T_{\text{max}}$  which depend on the current  $I_{\text{core}}$  and

temperature  $T_s$ . The relationship shows the complex heat transfer mechanism in the cable, which is formed by the change in the resistivity of the conductor when the temperature changes, combined with the limitation in the heat transfer capacity of the material layers.

In the current adjustment range from 200 A to 590 A, although the nonlinear heat transfer properties appear along the radial radius, leading to the difference between the temperature  $T_s$  and the temperature  $T_{max}$ , the simulation results still show a nearly linear correlation between the temperature  $T_s$  and the temperature  $T_{max}$ . Thereby, the method can bring practical applications, when the temperature  $T_{max}$  can be calculated based on the data collected from the temperature sensor  $T_s$ , allowing the prediction of the temperature distribution inside the cable. To test the reliability of the  $T_{max}$  temperature prediction model, the relative errors of  $T_{max}$  temperature from the linear regression equation and the simulation results were calculated at different operating current levels. The maximum relative errors occurred at current levels of 200 A, 300 A, 400 A, 500 A, and 590 A, which were 0.008%, 0.033%, 0.027%, 0.012%, and 0.002%, respectively. The obtained error magnitudes were relatively small, indicating that under the condition of changing operating current levels, the linear regression equation can provide an effective and relatively accurate prediction tool for estimating the  $T_{max}$  temperature of the insulation layer. This method is still quite feasible even considering the nonlinearity in the heat transfer of the cable.

Through the simulation results, the application of linear regression lines to determine the pair of temperature values ( $T_s$ ,  $T_{max}$ ) is an effective method to predict the warning threshold for the temperature parameter, corresponding to each specific operating level of the current. Fig. 7 shows in detail the intersections between the linear regression line and the fault axis  $T_{limit}$  of the graph in Fig. 5, in order to clarify the details and be able to determine the exact coordinates of the intersections. The intersection of the linear regression line of temperature with the threshold value axis  $T_{limit} = 90^\circ\text{C}$  allows to determine the warning temperature threshold  $T_s$  corresponding to the operating current level.

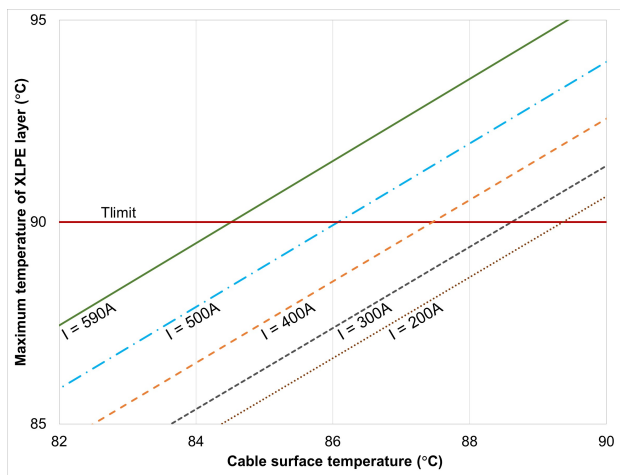


Fig. 7. The intersection point between the fitting temperature line and the operating limit temperature line of the XLPE insulation.

The value of  $T_{s,warning}$  is defined as the cable sheath surface temperature at which  $T_{max}$  reaches the allowable temperature limit  $T_{limit}$ . Using simulation,  $T_{s,warning}$  is calculated and shown in Table III, allowing us to determine the maximum cable sheath temperature at which the system needs to issue a warning to prevent overheating. Accurate calculation of  $T_{s,warning}$  is very important in cable temperature monitoring systems, allowing the system to detect overheating early before  $T_{max}$  reaches the dangerous threshold. This also helps prevent failure situations due to temperature exceeding the dielectric limit of the insulation material, thereby improving the reliability and service life of the cable.

TABLE III:  $T_{s,warning}$  VALUE AT DIFFERENT CURRENT LEVELS

$I$ (A)	200	300	400	500	590
$a$	1.002	1.004	1.008	1.012	1.017
$b$	0.457	1.030	1.839	2.889	4.046
$T_{s,warning}$ ( $^\circ\text{C}$ )	89.364	88.616	87.461	86.078	84.517

## V. CONCLUSION

Analyzing the temperature distribution in cable insulation is essential for early detection of potential failures. Temperature variations in the cable also cause changes in the electric field. Therefore, Simulation methods for determining cable temperature are crucial for evaluating the service life of cables under various operating conditions. This study investigated the temperature and electric field distribution in Medium Voltage (MV) cables over time using finite element simulations. The results highlight the critical impact of temperature variations on the cable's operational stability and lifespan. Key findings indicate that the temperature distribution within the cable reaches a steady state after approximately six hours of operation. The thermal behavior of the cable is influenced by the material layers, which regulate heat transfer and prevent localized overheating. Additionally, the electric field distribution is affected by temperature changes, with higher sheath temperatures leading to faster stabilization of the field but also posing a risk of electric field reversal. This underscores the importance of precise temperature monitoring to avoid insulation degradation and potential cable failures.

Furthermore, the study examined the relationship between sheath temperature ( $T_s$ ) and insulation temperature ( $T_{max}$ ) under different operating conditions. The nearly linear correlation between these variables allows for effective temperature predictions using linear regression models. The determination of a temperature warning threshold provides a practical approach for early fault detection. Specifically, when the cable operates at a rated current of 590 A, an alarm should be triggered when the sheath temperature reaches  $T_s=84.5^\circ\text{C}$ , ensuring preventive action before the insulation temperature exceeds the critical limit of  $90^\circ\text{C}$ .

The proposed temperature prediction and warning threshold models contribute to improving the reliability and longevity of MV cables. These findings can be applied in real-world power distribution systems to optimize cable installation, monitoring, and maintenance,

ultimately reducing the risk of failures due to thermal stress. Future research can expand upon this study by incorporating additional environmental factors and validating the models with experimental data.

#### CONFLICT OF INTEREST

The authors declare no conflicts of interest.

#### AUTHOR CONTRIBUTIONS

Quyen M. Hoang and Nga T. T. Vu formulated the basic idea for the integrated solution for temperature monitoring in the cable insulation, provided guidance and supervision throughout the research process and analysis. Hai D. Tran conducted simulations, completed the research, and writing this paper; all authors had approved the final version.

#### REFERENCES

- [1] D. He, T. Zhang, M. Ma, W. Gong, W. Wang and Q. Li, "Research on mechanical, physicochemical and electrical properties of XLPE-insulated cables under electrical-thermal aging," *Journal of Nanomaterials*, vol. 2020, no. 1, 2020. doi:10.1155/2020/3968737
- [2] R. Ullah and M. Akbar, "Lifetime estimation based on surface degradation and characterization of HTV silicone-rubber based composites for HVAC and HVDC transmission," *CSEE Journal of Power and Energy Systems*, vol. 9, no. 2, pp. 751–758, Mar. 2023.
- [3] Q. Wang, R. Liu, S. Qin, X. Chen, Z. Shen, Z. Hou, and Z. Ju, "Insulation properties and degradation mechanism for XLPE subjected to different aging periods," *CSEE Journal of Power and Energy Systems*, vol. 9, no. 5, pp. 1959–1967, 2023.
- [4] B. Liang, R. Lan, Q. Zang *et al.*, "Influence of thermal aging on dielectric properties of high voltage cable insulation layer," *Coatings*, vol. 13, no. 3, 2023. doi:10.3390/coatings13030527
- [5] A. Smaida, Y. Mecheri, L. Boukezzi *et al.*, "Mechanical behavior of 60 kV HV XLPE insulation under thermal aging and cross-correlation assessment of degradation mechanisms," *J. Mech. Sci. Technol.*, 2025. doi: 10.1007/s12206-025-0109-5
- [6] Y. Li, G. Zhen, Y. Liu *et al.*, "Effect of temperature on partial discharges activity and electrical trees propagation in XLPE," *IET Sci. Meas. Technol.*, vol. 18, no. 6, pp. 300–309, 2024.
- [7] Y. Liu, H. Xiong, and H. Xiao, "Detecting XLPE cable insulation damage based on distributed optical fiber temperature sensing," *Optical Fiber Technology*, vol. 68, 2022. doi: 10.1016/j.yofte.2021.102806
- [8] A. Henke and S. Frei, "Transient temperature calculation in a single cable using an analytic approach," *Journal of Fluid Flow, Heat and Mass Transfer*, vol. 7, 2020. doi: 10.11159/jffhmt.2020.006
- [9] Y. Zhang, F. Yu, Z. Ma, J. Li, J. Qian, X. Liang, J. Zhang, and M. Zhang, "Conductor temperature monitoring of high-voltage cables based on electromagnetic-thermal coupling temperature analysis," *Energies*, vol. 15, 2022. doi:10.3390/en15020525
- [10] J. Riba and J. Llauredó, "A model to calculate the current-temperature relationship of insulated and jacketed cables," *Materials*, vol. 15, no. 19, 2022. doi:10.3390/ma15196814
- [11] D. Enescu, P. Colella, and A. Russo, "Thermal assessment of power cables and impacts on cable current rating: An overview," *Energies*, vol. 13, no. 20, 2020. doi:10.3390/en13205319
- [12] J. H. Lienhard V and J. H. Lienhard IV, *A Heat Transfer Textbook*, 6th ed., Cambridge, MA: Phlogiston Press, 2024.
- [13] International Electrotechnical Commission, *Electric Cables—Calculation of the Current Rating*, IEC Standard 60287-1 and 60287-2-1, Geneva, Switzerland, 2023.
- [14] T. T. N. Vu, G. Teyssedre, B. Vissouvanadin *et al.*, "Correlating conductivity and space charge measurements in multi-dielectrics under various electrical and thermal stresses," *IEEE Trans. Dielectr. Electr. Insul.*, vol. 22, no. 1, pp. 117–127, 2015.

- [15] International Electrotechnical Commission, *Power Cables with Extruded Insulation and Their Accessories for Rated Voltages from 1 kV ( $U_m = 1.2$  kV) up to 30 kV ( $U_m = 36$  kV)—Part 2: Cables for Rated Voltages from 6 kV ( $U_m = 7.2$  kV) up to 30 kV ( $U_m = 36$  kV)*, IEC 60502-2, Geneva, Switzerland, 2014.
- [16] *Instructions of Choosing & Using Medium-voltage Cables*, Vietnam Electric Cable Corporation - CADIVI, 2022.
- [17] W. M. Haynes, *CRC Handbook of Chemistry and Physics*, 105th ed., Boca Raton: CRC Press, 2024.
- [18] J. E. Mark, *Polymer Data Handbook*, 2nd ed., Oxford University Press, 2023. doi:10.1093/oso/9780195181012.001.0001
- [19] H. Zhang, R. Ding, P. Lin, Y. Zeng, D. Lyu and G. Liu, "Application of thermal resistance dynamic characteristics on high-voltage cable ampacity based on field circuit coupling method," in *Proc. 2022 12th Int. Conf. on Power and Energy Systems (ICPES)*, Guangzhou, 2022, pp. 116–122.
- [20] A. S. Alghamdi and R. K. Desuqi, "A study of expected lifetime of XLPE insulation cables working at elevated temperatures by applying accelerated thermal ageing," *Heliyon*, vol. 6, no. 1, e03120, 2020, Jan. 2020.
- [21] S. Qin, Q. Xu, Q. Wang, J. Zhang, Z. Ju, Z. Hou, H. Lian, T. Wu, J. Zhang, "Study on temperature rise characteristics of 110 kV XLPE cable under different service years considering dielectric loss," *Energy Reports*, vol. 8, Sup. 8, 2022. doi: 10.1016/j.egy.2022.09.153

Copyright © 2025 by the authors. This is an open access article distributed under the Creative Commons Attribution License (CC BY 4.0), which permits use, distribution and reproduction in any medium, provided that the article is properly cited, the use is non-commercial and no modifications or adaptations are made.



**Quyen M. Hoang** was born in 1987 in Haiduong, Vietnam. He received the master's degree in electrical engineering from Grenoble University, France, in 2011. Then, He received the Ph.D. degree in electrical engineering from the University of Toulouse, France, in 2014. Currently, he is a lecturer at Hanoi University of Industry, Vietnam. The main research interests include solid insulating materials, applied physics, nanotechnology, energy, and sustainable development.



**Hai D. Tran** was born in 2001 in Thaibinh, Vietnam. The author received a bachelor's degree in 2023 and master's degree in 2025 in electrical engineering from Hanoi University of Industry, Vietnam. The main research interests are insulating materials, underground cable lines.



**Nga T. T. Vu** was born in 1981 in Hanoi, Vietnam. She received the master's degree in 2007 from the Hanoi University of Science and Technology, in Vietnam. She received the Ph.D. degree in electrical engineering from the University of Toulouse, France, in 2014 for a research work on space phenomena in polymeric insulating materials intended for HVDC cable application at the Laboratory of Plasma and Energy Conversion - Laplace in Toulouse, France. She has been working since 2004 as a researcher and lecturer at the Electric Power University in Hanoi, Vietnam.